International Journal of
Translational Medicine

MDPI

Article

Potential Translational Thioflavin T Methodology as a Complement of Cell-Based Assays and after Drug Exposition

Ana Salomé Correia [1,2], Diana Duarte [1,3], Vera Miranda-Gonçalves [2,4,5] and Nuno Vale [1,6,7,*]

1 OncoPharma Research Group, Center for Health Technology and Services Research (CINTESIS), Rua Dr. Plácido da Costa, s/n, 4200-450 Porto, Portugal; anncorr07@gmail.com (A.S.C.); dianaduarte29@gmail.com (D.D.)
2 Department of Pathology and Molecular Immunology, Institute of Biomedical Sciences Abel Salazar, University of Porto (ICBAS-UP), Rua Jorge Viterbo Ferreira 228, 4050-513 Porto, Portugal; vera.miranda.goncalves@ipoporto.min-saude.pt
3 Faculty of Pharmacy, University of Porto, Rua Jorge Viterbo Ferreira 228, 4050-513 Porto, Portugal
4 Cancer Biology and Epigenetics Group, IPO Porto Research Center (GEBC CI-IPOP), Portuguese Oncology Institute of Porto (IPO Porto), R. Dr. António Bernardino de Almeida, 4200-072 Porto, Portugal
5 Porto Comprehensive Cancer Center (P.CCC), R. Dr. António Bernardino de Almeida, 4200-072 Porto, Portugal
6 Department of Community Medicine, Information and Health Decision Sciences (MEDCIDS), Faculty of Medicine, University of Porto, Rua Dr. Plácido da Costa, s/n, 4200-450 Porto, Portugal
7 Associate Laboratory RISE-Health Research Network, Faculty of Medicine, University of Porto, Al. Prof. Hernâni Monteiro, 4200-319 Porto, Portugal
* Correspondence: nunovale@med.up.pt; Tel.: +351-22-042-6537

Abstract: Protein aggregation is a common characteristic of several human diseases such as Alzheimer's disease. Recent evidence has indicated that the aggregation of peptides such as p53 is also marked in cancer cells. The aim of this study was to correlate Thioflavin T (ThT) data with different cellular viability assays (Neutral Red and MTT) in SH-SY5Y neuroblastoma cells and HT-29 colon cancer cells treated with doxorubicin, a classical antineoplastic agent. We also studied the effects of the well-known peptide Aβ42 on the aggregation process in these cells. Our data suggest that both cancer cell lines are responsive to doxorubicin and formed aggregates, highlighting a relationship between ThT and cellular viability methodologies. We observed that lower values of cell viability corresponded with pronounced aggregation. Thus, these results indicated that the ThT methodology used in cells may complement the cell viability assays. In addition, this methodology may be of interest to evaluate the role of protein aggregation in other cancer cells.

Keywords: Thioflavin T; Aβ42; doxorubicin; SH-SY5Y cells; HT-29 cells

check for updates

Citation: Correia, A.S.; Duarte, D.; Miranda-Gonçalves, V.; Vale, N. Potential Translational Thioflavin T Methodology as a Complement of Cell-Based Assays and after Drug Exposition. *Int. J. Transl. Med.* **2022**, *2*, 134–147. https://doi.org/10.3390/ijtm2020011

Academic Editor: Pier Paolo Claudio

Received: 14 September 2021
Accepted: 18 March 2022
Published: 22 March 2022

Publisher's Note: MDPI stays neutral with regard to jurisdictional claims in published maps and institutional affiliations.

Copyright: © 2022 by the authors. Licensee MDPI, Basel, Switzerland. This article is an open access article distributed under the terms and conditions of the Creative Commons Attribution (CC BY) license (https://creativecommons.org/licenses/by/4.0/).

1. Introduction

In stressful situations, soluble proteins can undergo structural changes and self-assembly, culminating in their aggregation. Protein aggregation has been extensively studied and is pronounced in pathologies such as Parkinson's disease, Alzheimer's, and type 2 diabetes [1].

To monitor the in vitro formation of proteins and other aggregation structures, Thioflavin T (ThT) can be used. This molecule is a probe that—after binding to amyloid fibrils, hydrophobic pockets in globular proteins, and other molecules such as DNA oligomers—generates a fluorescent signal at 482 nm after excitation at 450 nm [2–4]. Although the phenomenon of protein aggregation has already been studied in cancer, the evaluation of the formation of aggregates by the ThT technique can generate information regarding cancer diagnosis and carcinogenesis processes [5]. For example, p53 aggregation can be an important factor in both carcinogenesis and tumour progression. The misfolded form of this protein can form amyloid-like fibrils, which ultimately lead to disturbances

in the pro-apoptotic and tumour-suppressing function of p53 [5,6]. Recently, a study also showed that breast cancer cells (MDA-MB-231 cell line) that are damaged at the mitochondrial level accumulate aggregates of p53 that resist degradation by lysosomes [7]. Evidence shows that this probe is also capable of binding nucleic acids [8] and recent studies have found that when using the ThT technique, it is also possible to detect microRNAs, known for being important biomarkers in various types of cancer [9]. Despite the advantages, there are several drawbacks associated with this methodology, particularly the lack of robustness. Additionally, the difficulty in finding optimal concentrations of ThT has generated a lack of consensus regarding the in vitro application of this probe [1]. In this manuscript, our research group aimed to understand whether the phenomenon of aggregation could be connected to cell viability studies (MTT and Neutral Red uptake assays) in the context of cancer. We then performed the ThT methodology on different cancer cell lines, HT-29 (colon cancer) and SH-SY5Y (neuroblastoma), after the application of a drug clinically used in cancer therapy, doxorubicin (DOXO). We then performed a comparison with the results obtained by the MTT and Neutral Red assays. Our results helped us to understand if the phenomenon of aggregation, detected by ThT, was important in cancer, if it was related to the viability of the cells, and if it varied in different types of cancer such as neuroblastoma and colon cancer. We demonstrated, for the first time, that the ThT methodology can be useful for studies involving peptides and cancer cells. In Figure 1, a summary of the methodologies used in this manuscript is represented.

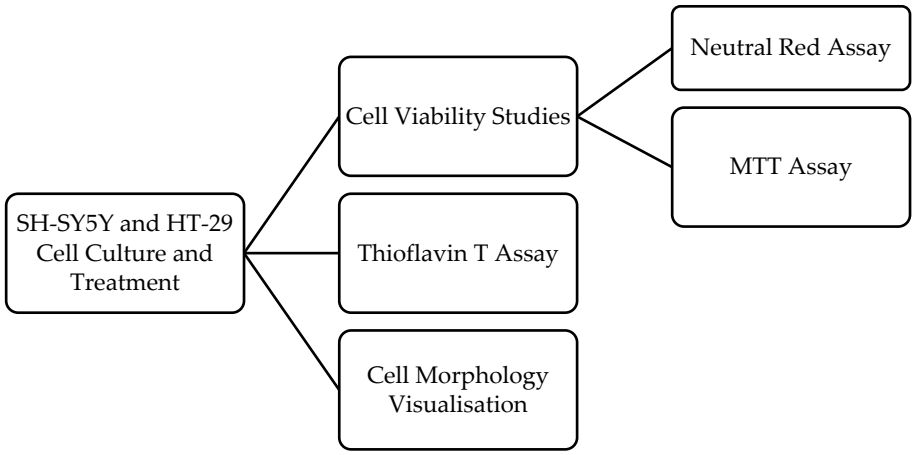

Figure 1. Summary of the methodologies used in this work.

2. Materials and Methods

2.1. Materials

Dulbecco's Modified Eagle's Medium (DMEM), foetal bovine serum (FBS), and penicillin-streptomycin mixture were obtained from Millipore Sigma (Merck KGaA, Darmstadt, Germany). Mccoy's 5A Medium, Thiazolyl Blue Tetrazolium Bromide (MTT; cat. no. M5655), a Neutral Red solution (cat. No. N2889), Thioflavin T (cat. no. T3516), and Hexafluoro-2-propanol (HFIP; cat. no. 105228) were purchased from Sigma-Aldrich (Merck KGaA, Darmstadt, Germany). Doxorubicin hydrochloride (cat. no. 2252) was purchased from Tocris Bioscience (Bristol, UK). The Aβ42 peptide (cat. no. RP20527) was purchased from GenScript (Piscataway, NJ, USA).

2.2. Cell Culture

Human neuroblastoma cell line SH-SY5Y (American Type Culture Collection, Manassas, VA, USA) and human colorectal adenocarcinoma cell line HT-29 (American Type Culture Collection, Massanas, VA, USA) were incubated at 37 °C in a humidified atmosphere (95% air, 5% CO_2). These cells were cultivated in DMEM and Mccoy's 5A Medium (SH-SY5Y cells and HT-29 cells, respectively) supplemented with 10% FBS and 1% of a

penicillin/streptomycin solution (1000 U/mL; 10 mg/mL). For culture maintenance, both cell lines were cultured in a monolayer and sub-cultured once a week when confluent (75–80%). Before each experiment, the cells were trypsinised (0.25% trypsin-EDTA), centrifuged (1100 rpm, 5 min), and seeded at a density of 1×10^5 cells/mL in 48-well plates, which were attached for a period of 24 h.

2.3. Cell Treatment

DOXO was dissolved in water (filtered) and added to both cell lines at final concentrations of 1 nM, 10 nM, 100 nM, 1 μM, and 10 μM. The cellular viability values were determined by MTT tetrazolium reduction and Neutral Red uptake assays after 24 h and 48 h of treatment with this drug, respectively. Dose-response curves and half-maximal inhibitory concentration (IC_{50}) values for this drug after 24 h and 48 h of treatment, respectively, were obtained through the Neutral Red uptake assay. For the preparation and incubation of the Aβ42 peptide in the cells, the peptide was dissolved in HFIP (1 mg/mL) and incubated overnight at room temperature. The peptide was then frozen (−80 °C) followed by lyophilisation to evaporate the HFIP. After this last process, the peptide was dissolved in water (1 mg/mL) and used in the cells at a concentration of 10 μM as previously described [10,11].

2.4. Cell Viability Assays

After the cells were attached to the 48-well plates, DOXO was applied to the cells for 24 h and 48 h. After the treatment with this agent, the cell viability was evaluated by two distinct assays, MTT and Neutral Red. For the MTT assay, the culture medium was discarded and 200 μL/well of MTT solution (0.5 mg/mL in PBS) was added to the cells. The cells were then incubated for 3 h (light-protected). After that, the MTT solution was removed and 200 μL/well of DMSO was added to the cells. The absorbance values (570 nm) were determined in an automated microplate reader (Tecan Infinite M200, Switzerland). For the Neutral Red uptake assay, the Neutral Red medium (1:100 in the culture medium) was prepared the day before; before being applied to the cells, this medium was centrifugated (10 min, 1800 rpm). After that, the cell culture medium was removed and 250 μL/well of Neutral Red solution was added to the cells followed by a period of incubation of 3 h (light-protected). This solution was then discarded, washed with PBS (300 μL/well), and 250 μL/well of Neutral Red de-stain solution (50% of 96% ethanol, 49% de-ionised water, and 1% glacial acetic acid) was added to the plate. The absorbance at 540 nm was determined in an automated microplate reader (Tecan Infinite M200, Tecan Group Ltd., Männedorf, Switzerland).

2.5. Cell Morphology Visualisation

After the treatments, the SH-SY5Y and HT-29 cell morphology was analysed using a Leica DMI6000B automated microscope (Wetzlar, Germany) coupled to a Leica DFC350 FX camera and LAS X software.

2.6. Thioflavin T Assay

After the cells were attached to the 48-well plates, DOXO and the Aβ42 peptide were applied to the cells for 24 h and 48 h. Both cell lines were then subjected to the Thioflavin T (ThT) assay to assess the cell staining with this dye. To perform this protocol, 300 μL/well of ThT (10 μM in PBS) was added to the cells (without aspiration). The plates were then subjected to a slight agitation for 10 min and the fluorescence (excitation 450 nm, emission 485 nm) was measured using a fluorescence microscope (Olympus IX51, Tokyo, Japan) coupled to an Olympus XM10 digital camera equipped with a FITC filter cube using CellSens software.

2.7. Statistical and Data Analyses

GraphPad Prism 8 software (San Diego, CA, USA) was used to create the graphs, calculate the IC_{50} values, and carry out the statistical analysis. The total cell counts and fluorescence quantification were performed using ImageJ software (version 1.6.1, National Institutes of Health; Bethesda, MD, USA). The results were presented as a mean ± SEM for a minimum of three independent experiments. Statistical comparisons were performed between the control and treatment conditions with a Student's *t*-test and a one-way ANOVA test. The differences were statistically significant when the *p*-value was < 0.05. Dose-response curves were obtained by non-linear regression (curve fit) using the function Y = 100/(1 + 10^([LogIC_{50}-X] * HillSlope)).

3. Results and Discussion

3.1. SH-SY5Y Cells and Peptide Aβ42

Our first aim was to observe the natural aggregation in human SH-SY5Y neuroblastoma cells based on morphological changes. The cell morphology of the untreated cells was assessed by phase-contrast microscopy (Figure 2A). Figure 2B represents the untreated cells stained with ThT and displaying background fluorescence.

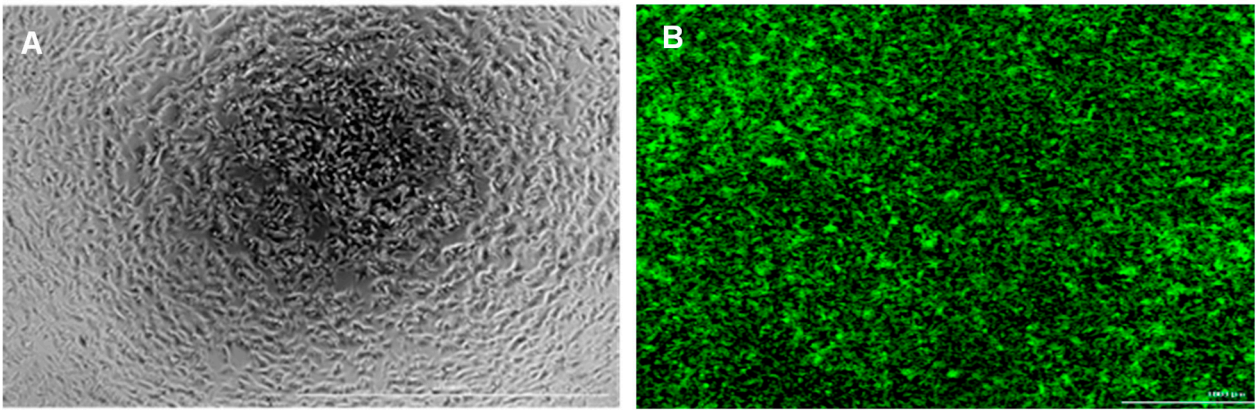

Figure 2. Phase-contrast images of untreated human SH-SY5Y cells (**A**) for 24 h and fluorescence images of untreated SH-SY5Y cells (**B**). Scale bar: 1020 µm.

Cell-penetrating peptides can be associated with the ability of aggregation and its sequence or cargo, and eventually cell death [12–23]. Human β-amyloid (1–42) peptide is a classical peptide used in studies of aggregation with ThT staining [24] because it is associated with the formation of protein aggregates. As shown in Table 1, the results demonstrated that this phenomenon of aggregation could be associated with the intrinsic properties associated with the protein structure such as the isoelectric point (5.17 for Aβ42). In Figure 3, the ratio of hydrophilic residues/total number of residues was close in the two peptides, representing an advantage.

3.2. Effect of Doxorubicin on the Viability of HT-29 and SH-SY5Y Cells

To explore the phenomenon of aggregation in neuroblastoma and colorectal cancer cells, and to understand if the ThT methodology could be used to complement cell viability assays such as MTT and NR, we started by treating SH-SY5Y and HT-29 cells with increasing concentrations of DOXO, a reference drug used for cancer therapy. This drug intercalates with DNA and inhibits the progression of topoisomerase II, impairing the synthesis of nucleic acids. After an exposition of 24 h and 48 h, the cell viability was evaluated by two different cell-based methods, MTT and Neutral Red (NR). The cell morphology was also evaluated by microscopy.

Table 1. Calculations and estimations on physiochemical properties of peptide Aβ42 using the software Pepcalc.com (peptide property calculator) [25] and the Peptide Calculator from BACHEM [26].

Peptide	Aβ42 (Beta-Amyloid Peptide (1–42) (Human))
Sequence	DAEFRHDSGYEVHHQKLVFFAEDVGSNKGAIIGLMVGGVVIA (COOH)
Number of residues	42
Molecular weight	4514.04 g/mol
Extinction coefficient	1280 M^{-1} cm^{-1}
Isoelectric point	pH 5.17
Net charge at pH 7	−2.7
Average hydrophilicity	−0.1
Ratio of hydrophilic residues/total number of residues	31%

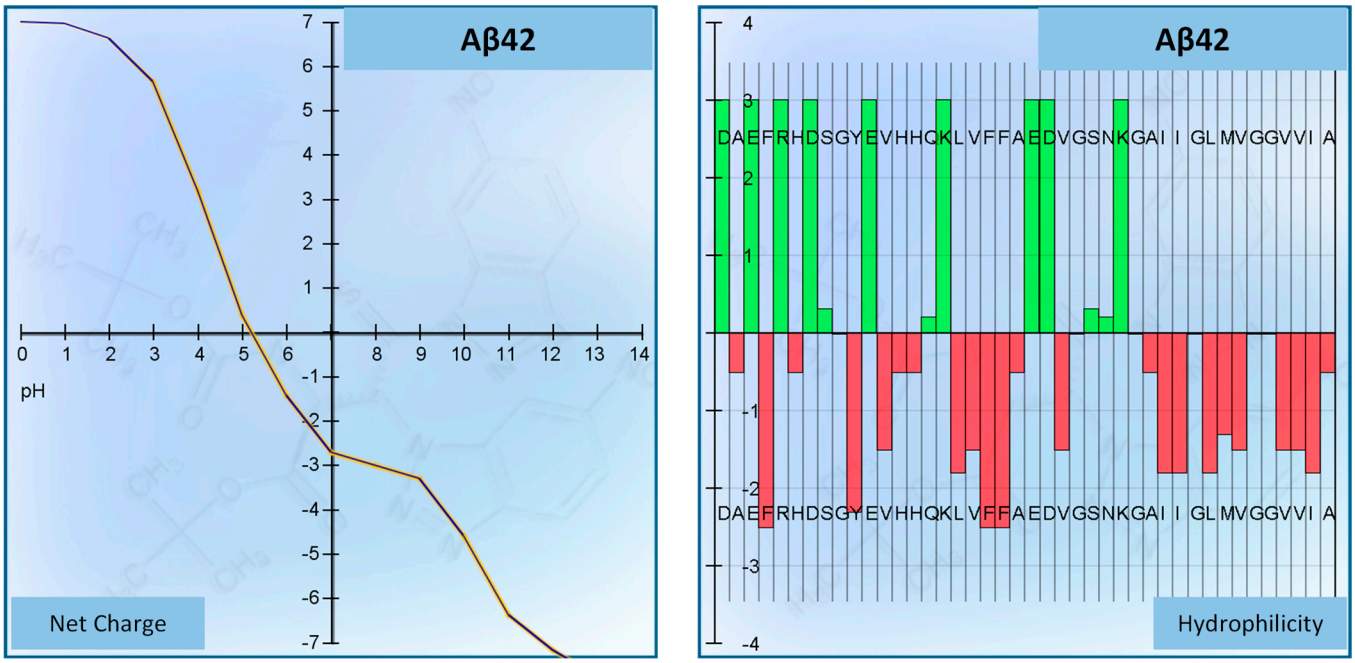

Figure 3. Representation of net charge and hydrophilicity of peptide Aβ42 (from Peptide Calculator/BACHEM).

For the HT-29 cells, the MTT results for the 24 h treatments demonstrated a lack of significant efficacy of DOXO in reducing the mitochondrial activity for all concentrations between 1 nM and 1 µM (Figure 4A). A significant reduction in the cell viability occurred in HT-29 treated with 10 µM of DOXO with a reduction of approximately 20% of the viable cells. The NR cytotoxicity assay was also used to evaluate the drug cytotoxicity as this technique is based on the ability of viable cells to take up Neutral Red via active transport and incorporate this dye into their lysosomes. The results for the NR assay agreed with the results obtained for the MTT assay and demonstrated the low activity of DOXO in the HT-29 cells except for the higher concentration (10 µM), whose treatment resulted in a decrease of almost 50% of the viable cells (Figure 4B). The dose-response curve for 24 h indicated that DOXO had an IC_{50} value of 1.473 µM (Figure 4C). These results were also observed by microscopy; there was a significant reduction in the cell numbers and changes in the morphology of the HT-29 cells treated with 10 µM DOXO, which became rounder and vacuolised (Figure S1).

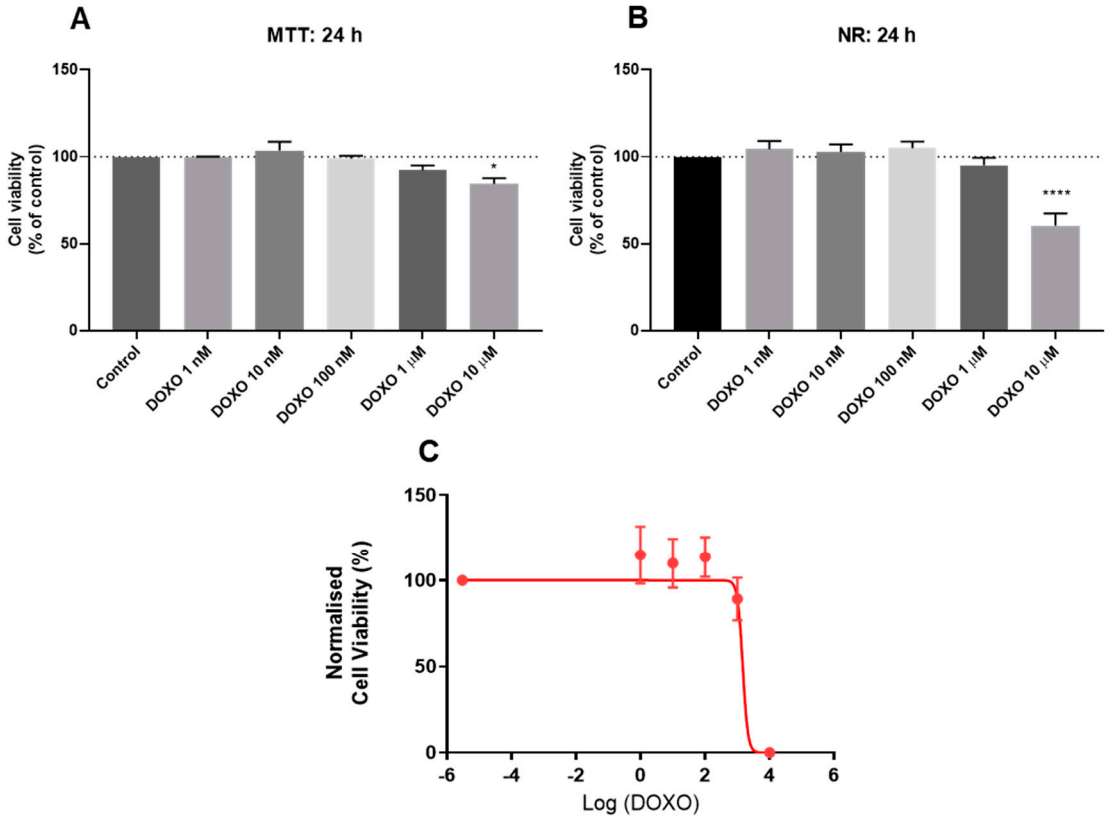

Figure 4. Effects of DOXO on the viability of HT-29 colon cancer cells determined by (**A**) MTT and (**B**) NR assays. Based on the results of the NR assay, a dose-response curve was calculated (**C**). Cells were treated with increasing concentrations of DOXO for 24 h. The results are shown as the percentage of the control and are expressed as the mean ± SEM of three independent experiments (n = 3). * Statistically significant vs. the control at $p < 0.05$. **** Statistically significant vs. the control at $p < 0.0001$.

To evaluate if prolonged exposure periods resulted in an enhanced efficacy of DOXO, we treated the HT-29 colon cell line for a period of 48 h with the same concentrations of DOXO as described above. The MTT results demonstrated a significant reduction in the cell viability in the concentrations of DOXO above 100 nM with 10 μM causing a reduction of 50% of the viable cells (Figure 5A). These results also agreed with the results obtained by the NR assay for 48 h (Figure 5B), validating both methodologies for the assessment of drug cytotoxicity. The IC_{50} for DOXO for 48 h was, as expected, lower than the one obtained for the 24 h treatment with a value of 801.7 nM (Figure 5C), demonstrating that the incubation time was a determinant for DOXO efficacy in the HT-29 cells. In accordance with these results, the cell morphology was also altered compared with the control cells in the treatments with DOXO above 100 nM with the cells becoming more vacuolised and rounder and forming fewer aggregates (Figure S2).

Regarding the SH-SY5Y cells, these cells were responsive to DOXO and, in general, the cell viability was inversely proportional to the concentration values of DOXO at both 24 h (Figures 6 and S3) and 48 h (Figures 7 and S4). This response was more pronounced after 48 h of treatment (Figure 7), andin the Neutral Red assay (Figures 6B and 7B), compared with the MTT assay (Figures 6A and 7A). These results were in agreement with the obtained results for the HT-29 cells and both methodologies for the assessment of drug cytotoxicity were validated. The lowest values of cellular viability were obtained for concentrations greater than 100 nM, which were statistically significant vs. the control. By analysing the obtained dose-response curves, it was possible to observe that with concentrations of 118.5 nM (Figure 6C) and 91.91 nM (Figure 7C), there was a reduction of 50% of the cells. These values of concentration represented the IC_{50} values of DOXO on the SH-SY5Y cells for 24 h and 48 h, respectively. Analysing Figures S3 and S4, it was possible to verify that

higher concentrations of DOXO resulted in a smaller number of cells, a greater number of damaged cells, and more rounded morphologies, which are characteristics of non-viable cells. After 48 h of drug exposure and with concentrations greater than 100 nM, this effect was even more pronounced, in agreement with the viability assays.

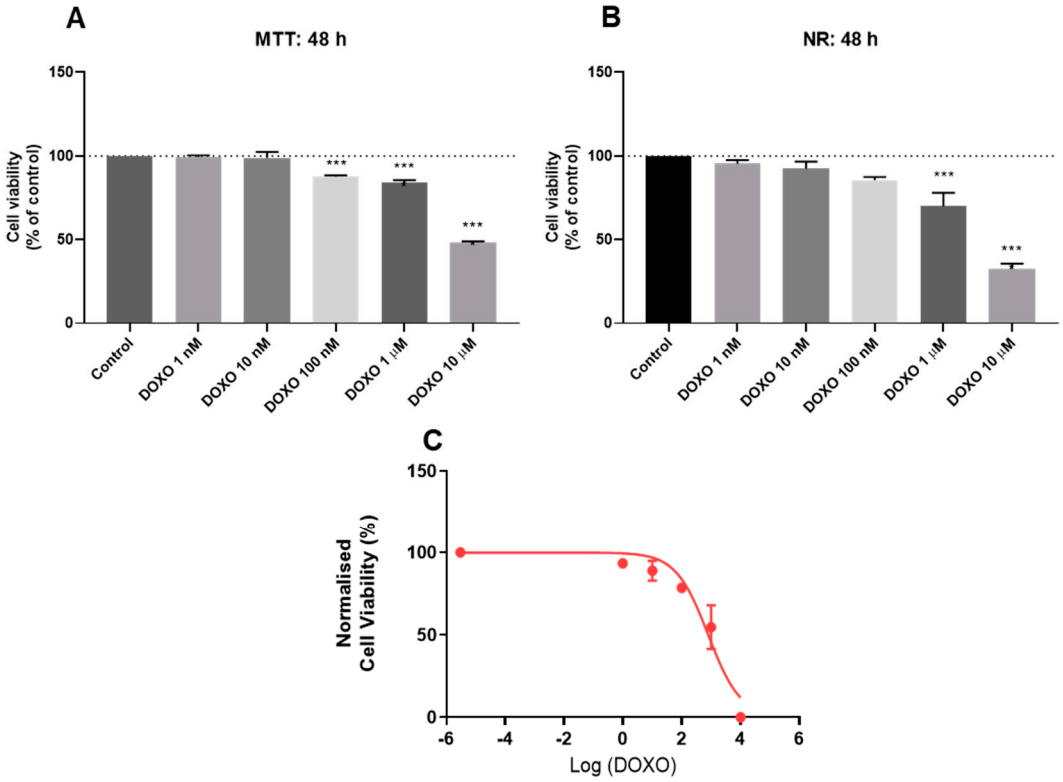

Figure 5. Effects of DOXO on the viability of HT-29 colon cancer cells determined by (**A**) MTT and (**B**) NR assays. Based on the results of the NR assay, a dose-response curve was calculated (**C**). Cells were treated with increasing concentrations of DOXO for 48 h. The results are shown as the percentage of the control and are expressed as the mean ± SEM of three independent experiments (n = 3). *** Statistically significant vs. the control at $p < 0.001$.

Taken together, these results supported the antineoplastic activity of DOXO in the HT-29 and SH-SY5Y cell lines.

3.3. Effect of Doxorubicin on the Thioflavin T Staining of HT-29 and SH-SY5Y Cells

We then evaluated the formation of aggregates in HT-29 colorectal cancer cells and SH-SY5Y neuroblastoma cells expressed in relative fluorescence units (RFU; fold change vs. the control cells) using the ThT methodology over 24 h and 48 h with a DOXO treatment. The Aβ42 peptide was also used as a positive control.

Regarding the SH-SY5Y neuroblastoma cells, our results revealed that between the concentrations of 1 nM and 1 µM of DOXO, the fluorescence intensity increased at both 24 h (Figure 8A) and 48 h (Figure 8B). This growing trend was even more pronounced at 48 h of treatment. Of all the concentrations, the treatment with 1 µM of DOXO led to the highest RFU values (Figure 9), especially at 48 h. Due to the interference of the strong reddish solution of 10 µM of DOXO, there was a significant amount of background noise in the fluorescent images and the evaluation of the relative fluorescence could not accurately be ascertained for this concentration.

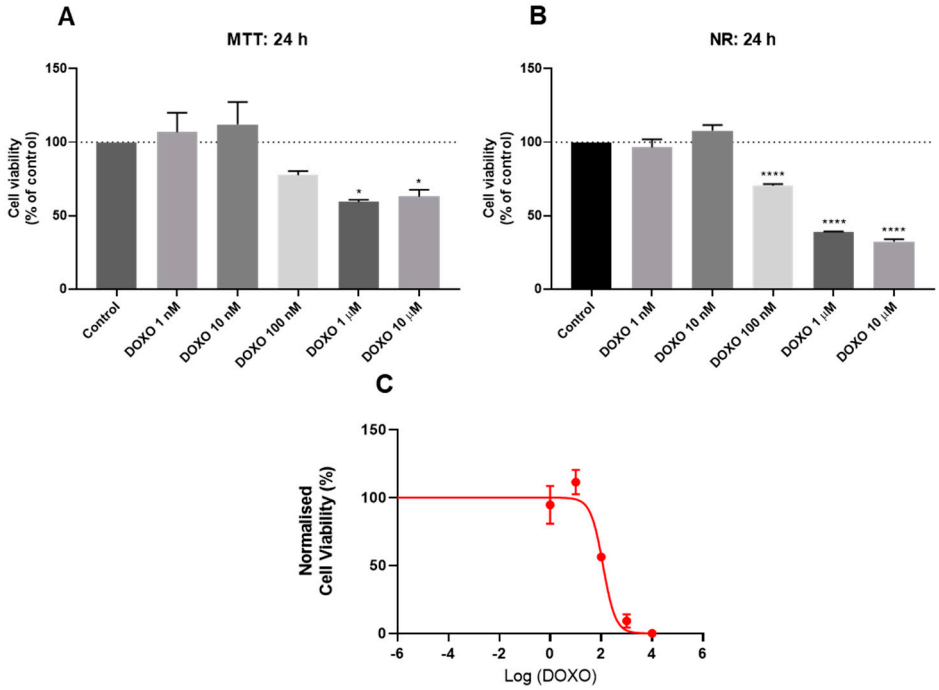

Figure 6. Effects of DOXO on the viability of SH-SY5Y neuroblastoma cells determined by (**A**) MTT and (**B**) NR assays. Based on the results of the NR assay, a dose-response curve was calculated (**C**). Cells were treated with increasing concentrations of DOXO for 24 h. The results are shown as the percentage of the control and are expressed as the mean ± SEM of three independent experiments ($n = 3$). * Statistically significant vs. the control at $p < 0.05$. **** Statistically significant vs. the control at $p < 0.0001$.

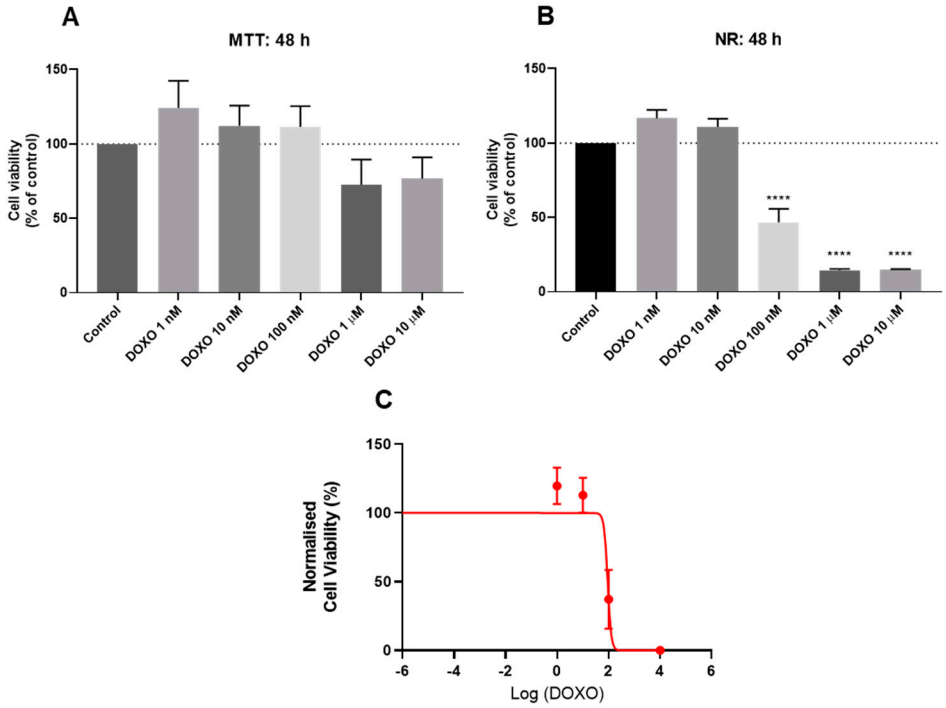

Figure 7. Effects of DOXO on the viability of SH-SY5Y neuroblastoma cells determined by (**A**) MTT and (**B**) NR assays. Based on the results of the NR assay, a dose-response curve was calculated (**C**). Cells were treated with increasing concentrations of DOXO for 48 h. The results are shown as the percentage of the control and are expressed as the mean ± SEM of four independent experiments ($n = 4$). **** Statistically significant vs. the control at $p < 0.0001$.

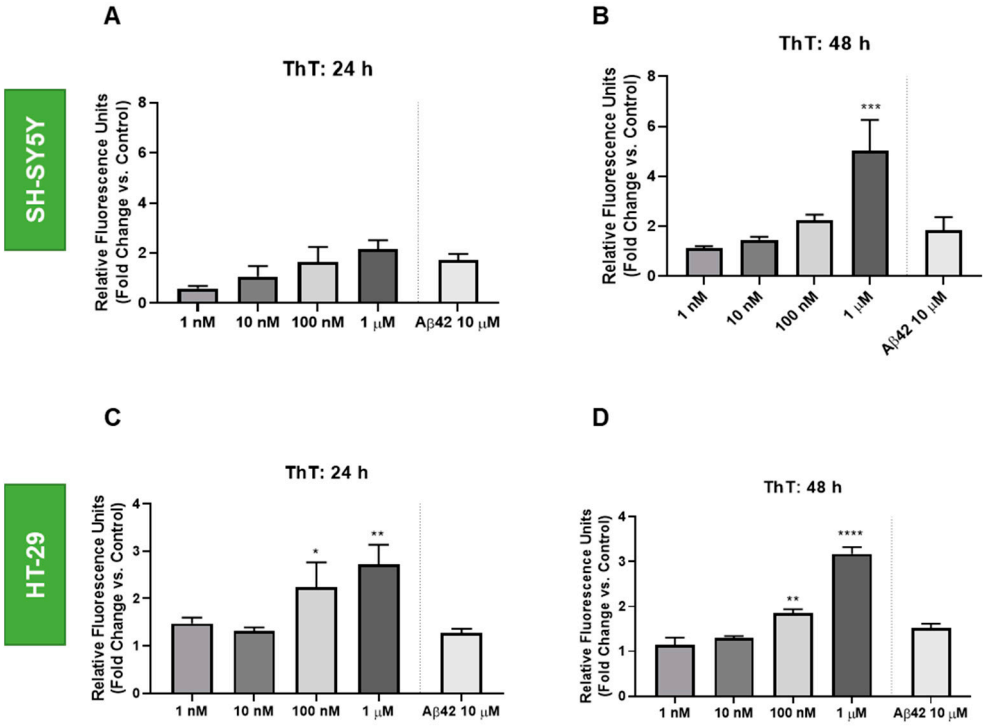

Figure 8. Effects of treatment with DOXO on the formation of aggregates in SH-SY5Y neuroblastoma cells (**A**,**B**) and HT-29 colon cancer cells (**C**,**D**) for 24 h (left) and 48 h (right) treatments. Cells were stained with ThT and aggregate formation was quantified in relative fluorescence units. Cells were treated with increasing concentrations of DOXO. Aβ42 peptide was added as a positive control. The results are shown as a fold change vs. the control and are expressed as the mean ± SEM of three independent experiments (n = 3). * Statistically significant vs. the control at $p < 0.05$. ** Statistically significant vs. the control at $p < 0.01$. *** Statistically significant vs. the control at $p < 0.001$. **** Statistically significant vs. the control at $p < 0.0001$.

Regarding the HT-29 cells, for the 24 h treatment (Figure 8C), there was a concentration-dependent increase in the fluorescence among all concentrations. The highest value of fluorescence was obtained in the treatments with 1 μM of DOXO (Figure 9). For the 48 h treatment (Figure 8D), there was less fluorescence signal per treatment compared with the treatments for 24 h. The relative fluorescence followed the same tendency as the treatment for 24 h with the highest value for the 1 μM DOXO treatment. Regarding the results obtained with the Aβ42 peptide, it led to a higher RFU vs. the control. However, in general, the fluorescence values obtained for this peptide were lower than those obtained for the treatment of the cells with DOXO. Taken together, our results for both cell lines and both periods of treatment demonstrated that DOXO could induce a greater formation of aggregates than the positive control (Aβ42).

Comparing the MTT and NR assays with the ThT methodology, we observed that lower values of cellular viability correlated with greater aggregation both in SH-SY5Y (Figure 10A,B) and HT-29 (Figure 10C,D) for treatments of 24 and 48 h. Our results suggested that the ThT methodology used in the cells could complement cell viability assays such as MTT and NR. Using this methodology, it was possible to hypothesise that an increase in DOXO concentrations (and periods of incubation) led to more significant cellular changes and toxicity, allowing ThT to easily gain access to compromised cells. These results allowed us to establish a relationship between ThT and cellular viability assays.

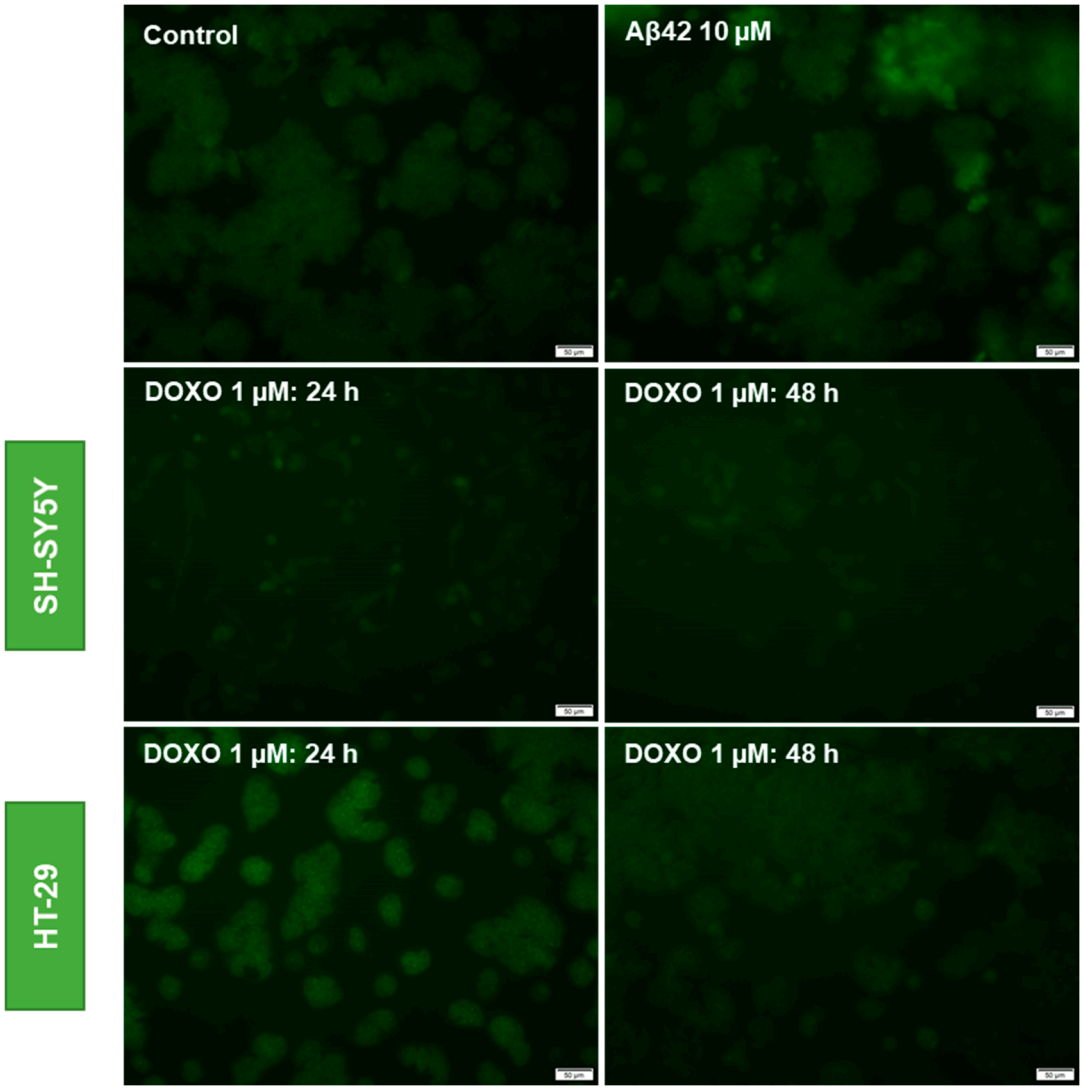

Figure 9. Images of the formation of aggregates in SH-SY5Y neuroblastoma cells and HT-29 colon cancer cells treated with DOXO (1 μM). Cells were stained with ThT. Aβ42 peptide was added as a positive control. Representative images were obtained in three independent experiments (n = 3). Scale bar: 50 μm.

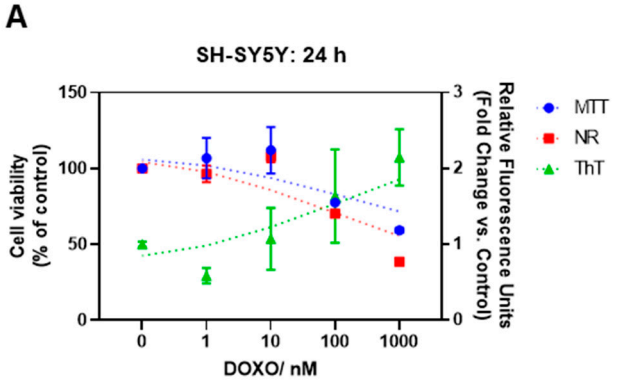

Figure 10. *Cont.*

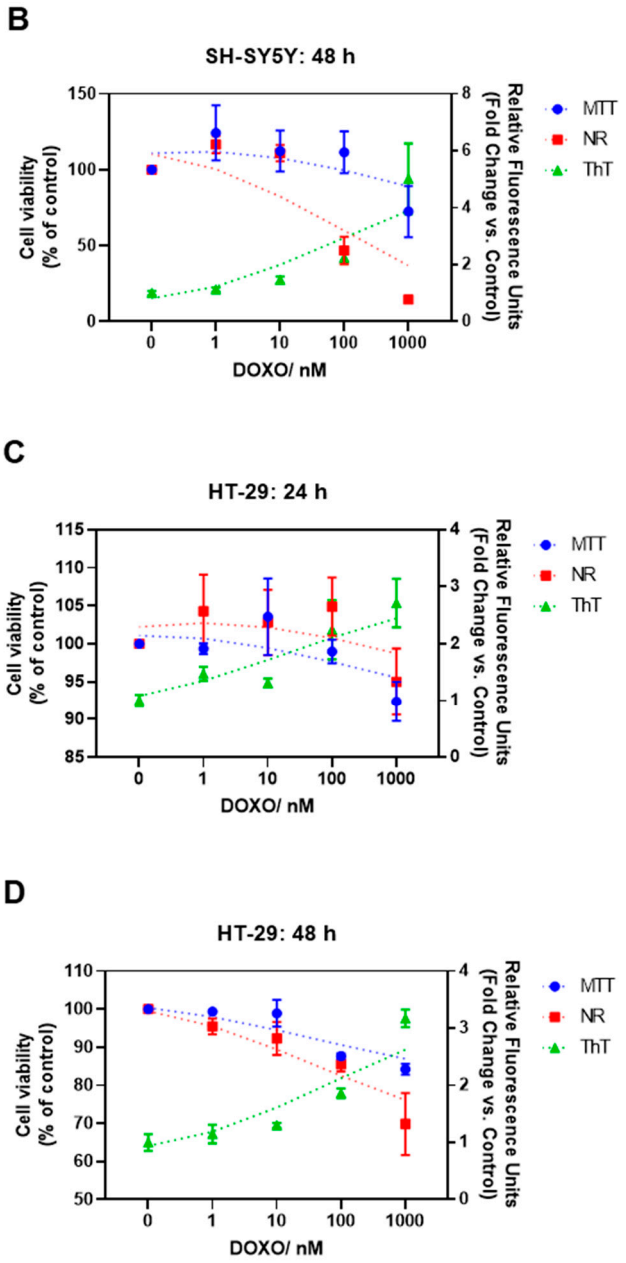

Figure 10. Relationship between MTT, NR, and ThT results obtained in two different cell lines, SH-SY5Y neuroblastoma (**A**,**B**) and HT-29 colon cancer cells (**C**,**D**) treated with DOXO for 24 and 48 h, respectively.

4. Conclusions

Protein aggregation is a frequent characteristic in many neurodegenerative pathologies. Recently, this process was also associated with carcinogenesis. Therefore, the analysis of protein or other structures and aggregation in cancer cells may be a relevant additional parameter for a detailed characterisation of cancer status. Thus, the major aim of the present study was to determine the formation of aggregates in cancer cells (SH-SY5Y cells and HT-29 cells) by a ThT assay and link these data with cellular viability data after treatment with DOXO. Our data indicated that in both cancer cell lines, the increase in the effectiveness of DOXO accompanied a loss of viability of the cells. One of these factors could be associated with aggregation phenomena, which was confirmed by our data obtained with the Thioflavin T method. Our data also revealed that the Thioflavin methodology had a different affinity according to the period of contact of the cells with the drug and the type

of cell. However, in both cancer cell lines in the study, there was a similar tendency of an RFU increase that followed a cellular viability decrease. It is important to mention that the observed fluorescence after the ThT application could be explained by the presence of amyloid aggregates, globular proteins, other compounds such as DNA oligomers, or other non-amyloid structures because, as mentioned in the introductory section, ThT also reflects the presence of other molecules. In summary, with the application of DOXO in crescent concentrations, we observed that lower cell viability values correlated with greater fluorescence values obtained with the ThT methodology. As it has already been extensively described and demonstrated in this manuscript, DOXO is a drug that is cytotoxic but in a different way from the Aβ42 peptide and tends to lead to neurodegeneration/apoptosis in a time-consuming process, which may explain the differences observed between DOXO and the Aβ42 peptide, mainly regarding cytotoxicity [27]. Thus, these data can provide evidence about a connection between the cell viability values by MTT/NR approaches and the fluorescence values by the ThT methodology. Greater cytotoxicity reflects in greater ThT fluorescence. Nevertheless, these results allow the study of aggregation in the context of cancer because there is a strong possibility that DOXO may trigger a few pathways involved in aggregation such as p53 aggregation [28]. Further studies regarding the Thioflavin T technique may be necessary to study the role of protein aggregation in other cancer cells because this technique may be very important to complete other methodologies and provide further details regarding cancer evolution and carcinogenesis processes. Future research should determine the co-localisation of ThT dye and other relevant proteins in the context of cancer such as p53 protein.

Supplementary Materials: The following supporting information can be downloaded at https://www.mdpi.com/article/10.3390/ijtm2020011/s1; Figure S1: Effects of 24 h treatment with DOXO on the morphology of HT-29 cells. Representative images obtained in three independent experiments (n = 3). Scale bar: 50 μM; Figure S2: Effects of 48 h treatment with DOXO on the morphology of HT-29 cells. Representative images obtained in three independent experiments (n = 3). Scale bar: 50 μm; Figure S3: Effects of 24 h treatment with DOXO on the morphology of SH-SY5Y cells. Representative images obtained in three independent experiments (n = 3). Scale bar: 50 μm; Figure S4: Effects of 48 h treatment with DOXO on the morphology of SH-SY5Y cells. Representative images obtained in three independent experiments (n = 3). Scale bar: 50 μm.

Author Contributions: Conceptualisation, N.V.; methodology, D.D. and A.S.C.; formal analysis, A.S.C., D.D. and N.V.; investigation, A.S.C., D.D., V.M.-G. and N.V.; resources, V.M.-G. and N.V.; writing—original draft preparation, A.S.C. and D.D.; writing—review and editing, A.S.C., D.D. and N.V.; supervision, N.V.; project administration, N.V.; funding acquisition, N.V. All authors have read and agreed to the published version of the manuscript.

Funding: This research was financed by Fundo Europeu de Desenvolvimento Regional (FEDER) funds through the COMPETE 2020 Operational Programme for Competitiveness and Internationalisation (POCI), Portugal 2020, and by Portuguese funds through Fundação para a Ciência e a Tecnologia (FCT) in the framework of the project IF/00092/2014/CP1255/CT0004 and CHAIR in Onco-Innovation.

Institutional Review Board Statement: Not applicable.

Informed Consent Statement: Not applicable.

Data Availability Statement: Not applicable.

Acknowledgments: This article was supported by National Funds through Fundação para a Ciência e a Tecnologia (FCT), I.P., within CINTESIS, R & D Unit (reference UIDB/4255/2020). Diana Duarte acknowledges FCT for funding her PhD grant (SFRH/BD/140734/2018). Ana Correia acknowledges FCT for funding her PhD grant (SFRH/BD/146093/2019).

Conflicts of Interest: The authors declare no conflict of interest.

References

1. Xue, C.; Lin, T.Y.; Chang, D.; Guo, Z. Thioflavin T as an amyloid dye: Fibril quantification, optimal concentration and effect on aggregation. *R. Soc. Open Sci.* **2017**, *4*, 160696. [CrossRef]
2. Mohanty, J.; Barooah, N.; Dhamodharan, V.; Harikrishna, S.; Pradeepkumar, P.I.; Bhasikuttan, A.C. Thioflavin T as an efficient inducer and selective fluorescent sensor for the human telomeric G-quadruplex DNA. *J. Am. Chem. Soc.* **2013**, *135*, 367–376. [CrossRef]
3. Harel, M.; Sonoda, L.K.; Silman, I.; Sussman, J.L.; Rosenberry, T.L. Crystal Structure of Thioflavin T Bound to the Peripheral Site of Torpedo californica Acetylcholinesterase Reveals How Thioflavin T Acts as a Sensitive Fluorescent Reporter of Ligand Binding to the Acylation Site. *J. Am. Chem. Soc.* **2008**, *130*, 7856–7861. [CrossRef]
4. LeVine, H. Quantification of β-sheet amyloid fibril structures with thioflavin T. In *Methods in Enzymology*; Academic Press Inc.: Cambridge, MA, USA, 1999; Volume 309, pp. 274–284.
5. Takamatsu, Y.; Ho, G.; Hashimoto, M. Amyloid Evolvability and Cancer. *Trends Cancer* **2020**, *6*, 624–627. [CrossRef]
6. Yang-Hartwich, Y.; Bingham, J.; Garofalo, F.; Alvero, A.B.; Mor, G. Detection of p53 Protein Aggregation in Cancer Cell Lines and Tumor Samples. In *Methods in Molecular Biology*; Humana Press Inc.: Totowa, NJ, USA, 2015; Volume 1219, pp. 75–86.
7. Biel, T.G.; Aryal, B.; Gerber, M.H.; Trevino, J.G.; Mizuno, N.; Rao, V.A. Mitochondrial dysfunction generates aggregates that resist lysosomal degradation in human breast cancer cells. *Cell Death Dis.* **2020**, *11*, 460. [CrossRef] [PubMed]
8. Yeasmin Khusbu, F.; Zhou, X.; Chen, H.; Ma, C.; Wang, K. Thioflavin T as a fluorescence probe for biosensing applications. *TrAC Trends Anal. Chem.* **2018**, *109*, 1–18. [CrossRef]
9. Fan, T.; Mao, Y.; Liu, F.; Zhang, W.; Yin, J.; Jiang, Y. Dual signal amplification strategy for specific detection of Circulating microRNAs based on Thioflavin T. *Sens. Actuators B Chem.* **2017**, *249*, 1–7. [CrossRef]
10. Zatsepina, O.G.; Kechko, O.I.; Mitkevich, V.A.; Kozin, S.A.; Yurinskaya, M.M.; Vinokurov, M.G.; Serebryakova, M.V.; Rezvykh, A.P.; Evgen'Ev, M.B.; Makarov, A.A. Amyloid-β with isomerized Asp7 cytotoxicity is coupled to protein phosphorylation. *Sci. Rep.* **2018**, *8*, 3518. [CrossRef]
11. Gibbs, E.; Silverman, J.M.; Zhao, B.; Peng, X.; Wang, J.; Wellington, C.L.; Mackenzie, I.R.; Plotkin, S.S.; Kaplan, J.M.; Cashman, N.R. A Rationally Designed Humanized Antibody Selective for Amyloid Beta Oligomers in Alzheimer's Disease. *Sci. Rep.* **2019**, *9*, 9870. [CrossRef]
12. Oehlke, J.; Scheller, A.; Wiesner, B.; Krause, E.; Beyermann, M.; Klauschenz, E.; Melzig, M.; Bienert, M. Cellular uptake of an α-helical amphipathic model peptide with the potential to deliver polar compounds into the cell interior non-endocytically. *Biochim. Biophys. Acta-Biomembr.* **1998**, *1414*, 127–139. [CrossRef]
13. Oehlke, J.; Wallukat, G.; Wolf, Y.; Ehrlich, A.; Wiesner, B.; Berger, H.; Bienert, M. Enhancement of intracellular concentration and biological activity of PNA after conjugation with a cell-penetrating synthetic model peptide. *Eur. J. Biochem.* **2004**, *271*, 3043–3049. [CrossRef]
14. Kenien, R.; Shen, W.-C.; Zaro, J.L. Vesicle-to-cytosol transport of disulfide-linked cargo mediated by an amphipathic cell-penetrating peptide. *J. Drug Target.* **2012**, *20*, 793–800. [CrossRef] [PubMed]
15. Scheller, A.; Melzig, M.; Oehlke, J. Induction of caspase-8 in human cells by the extracellular administration of peptides containing a C-terminal SLV sequence. *Lett. Pept. Sci.* **2001**, *8*, 29–34. [CrossRef]
16. Hällbrink, M.; Florén, A.; Elmquist, A.; Pooga, M.; Bartfai, T.; Langel, Ü. Cargo delivery kinetics of cell-penetrating peptides. *Biochim. Biophys. Acta-Biomembr.* **2001**, *1515*, 101–109. [CrossRef]
17. Silva, S.; Alves, C.; Duarte, D.; Costa, A.; Sarmento, B.; Almeida, A.J.; Gomes, P.; Vale, N. Model Amphipathic Peptide Coupled with Tacrine to Improve Its Antiproliferative Activity. *Int. J. Mol. Sci.* **2021**, *22*, 242. [CrossRef]
18. Yang, V.; Pedrosa, S.S.; Fernandes, R.; Maurício, A.C.; Koksch, B.; Gärtner, F.; Amorim, I.; Vale, N. Synthesis of PEGylated methotrexate conjugated with a novel CPP6, in sillico structural insights and activity in MCF-7 cells. *J. Mol. Struct.* **2019**, *1192*, 201–207. [CrossRef]
19. Silva, S.; Santos-Silva, A.; da Costa, J.M.C.; Vale, N. Potent cationic antimicrobial peptides against Mycobacterium tuberculosis in vitro. *J. Glob. Antimicrob. Resist.* **2019**, *19*, 132–135. [CrossRef]
20. Duarte, D.; Fraga, A.G.; Pedrosa, J.; Martel, F.; Vale, N. Increasing the potential of cell-penetrating peptides for cancer therapy using a new pentagonal scaffold. *Eur. J. Pharmacol.* **2019**, *860*, 172554. [CrossRef]
21. Ferreira, A.; Lapa, R.; Vale, N. Combination of Gemcitabine with Cell-Penetrating Peptides: A Pharmacokinetic Approach Using In Silico Tools. *Biomolecules* **2019**, *9*, 693. [CrossRef]
22. Correia, C.; Xavier, C.P.R.R.; Duarte, D.; Ferreira, A.; Moreira, S.; Vasconcelos, M.H.; Vale, N. Development of potent CPP6–gemcitabine conjugates against human prostate cancer cell line (PC-3). *RSC Med. Chem.* **2020**, *11*, 268–273. [CrossRef]
23. Silva, S.; Marto, J.; Gonçalves, L.; Almeida, A.J.; Vale, N. Formulation, Characterization and Evaluation against SH-SY5Y Cells of New Tacrine and Tacrine-MAP Loaded with Lipid Nanoparticles. *Nanomaterials* **2020**, *10*, 2089. [CrossRef]
24. Bourhim, M.; Kruzel, M.; Srikrishnan, T.; Nicotera, T. Linear quantitation of Aβ aggregation using Thioflavin T: Reduction in fibril formation by colostrinin. *J. Neurosci. Methods* **2007**, *160*, 264–268. [CrossRef] [PubMed]
25. PepCalc.com-Peptide Calculator. Available online: https://pepcalc.com/ (accessed on 14 September 2021).
26. Peptide Calculator. Available online: https://www.bachem.com/knowledge-center/peptide-calculator/ (accessed on 14 September 2021).

27. Han, X.-J.; Hu, Y.-Y.; Yang, Z.-J.; Jiang, L.-P.; Shi, S.-L.; Li, Y.-R.; Guo, M.-Y.; Wu, H.-L.; Wan, Y.-Y. Amyloid β-42 induces neuronal apoptosis by targeting mitochondria. *Mol. Med. Rep.* **2017**, *16*, 4521–4528. [CrossRef] [PubMed]
28. Garg, A.; Sinha, S. Doxorubicin induces Aberrant Self-Assembly of P53 by Phase Separation. *Biophys. J.* **2021**, *120*, 28a. [CrossRef]